

Investigation of Resonant Overvoltages in Offshore Wind Farms- Modeling and Protection

Amir Hayati Soloot, Himanshu J. Bahirat, Hans Kristian Høidalen, Bjørn Gustavsen and Bruce A. Mork

Abstract— Earth fault and switching operation may lead to resonant overvoltages in Offshore Wind Farms (OWF) with higher amplitude and rate of rise (du/dt) compared to other overvoltages. Overvoltages appear on High Voltage (HV) cables and Low Voltage (LV) side of wind turbines, and can result in insulation failure of the Wind Turbine Transformers (WTTs), interconnecting cables and Power Converters (PC). This paper aims to study the circumstance of the occurrence of these overvoltages and suggests proper protection methods.

This paper uses high frequency black box model for WTT. The power converter is modeled with two back to back voltage source converters. The RL harmonic filters and snubber circuits are included. This model can simulate the steady state operation as well as resonant overvoltage due to earth fault in ATP-EMTP software. But, it requires long simulation time. A simplified model which has the same accuracy as the first model for resonant transient is introduced.

Simulation results show that the transferred overvoltages to LV side due to earth fault at critical cable lengths may lead to resonant overvoltages with amplitude and rate of rise up to 30 p.u. and 400 p.u./ μ s, respectively. It is also shown that the installation of surge arresters at LV and HV terminal of WTTs only decreases the amplitude of overvoltages to safe margin and not the du/dt . However, the application of RC filters instead of surge arresters can protect offshore wind farm components from overvoltages.

Keywords: offshore wind farm, wind farm energization, earth fault, power converter, wind turbine transformers, RC filters.

I. INTRODUCTION

DUE to the recent focus of power operating and Transmission & Distribution (T&D) companies on offshore wind farm installations as a renewable energy solution, the maintenance and protection of the wind power components have become of great importance. The challenges of accessibility and repair require more effective protective devices compared to land-based wind farms. In literature,

This work was supported by the Norwegian Research Center for Offshore Wind Farm (NOWITECH)-Work package (4).

A. H. Soloot and H. K. Høidalen are with the Department of Electrical Power Engineering, Norwegian University of Science and Technology (NTNU), Trondheim N-7491, Norway (e-mail: amir.h.soloot@elkraft.ntnu.no, hans.hoidalen@elkraft.ntnu.no).

H. J. Bahirat and B. A. Mork are with the Department of Electrical and Computer Engineering, Michigan Technological University, Houghton, MI 49931 USA (e-mail: hjbahira@mtu.edu, bamork@mtu.edu).

B. Gustavsen is with SINTEF Energy Research, Trondheim N-7465, Norway (e-mail: bjorn.gustavsen@sintef.no).

Paper submitted to the International Conference on Power Systems Transients (IPST2013) in Vancouver, Canada July 18-20, 2013.

switching transients in land-based wind farms and OWFs [1]-[8] have been studied and analyzed, mainly concentrated on transients in the HV interconnecting grid. Different aspects are discussed such as the inrush current [1,2], the energization overvoltages on HV terminal of WTTs and inside winding [2,3,6,7,8] and earth fault interruption challenges in the adjacent network [2,4,5,6,7]. However, there have been few studies on the transferred resonant overvoltage to LV side [8]. Thus, the motivation of this paper is to study the transient overvoltages, mainly resonant overvoltage, transferred to LV terminal of WTT. Besides, the effect of protective devices, such as surge arrester and RC filters are analyzed.

The energization of each wind turbine may result in cable-transformer resonant transients. The length of cables in wind turbines typically are such that their quarter wave frequency can match resonance frequencies of WTTs. The resonant overvoltages may lead to internal insulation failures in transformers. Resonant overvoltages can also occur due to earth fault in cables or joints. In this case, they can be harmful for the connected power converters at LV terminal as well.

Typical components in offshore wind farms are modeled in this paper considering the high frequency content of the involved transients. In this paper, the model of a typical OWF is explained in section II. The simulation results for energization and earth fault transients are analyzed in section III.

II. OFFSHORE WIND FARM MODELING

The OWF considered for simulations is illustrated in Fig. 1. Several wind farm rows are connected to each winding of platform transformer. Each row consists of several WTTs connected with the HV cables. There are Vacuum Circuit Breakers (VCBs) to switch each WTTs and one VCB for switching the entire row. In the LV side, full-scale frequency converters are installed. The power converters are initiated after the energization of WTTs. Therefore, they are off and can be disregarded. However, during earth fault, the wind turbines are producing power and power converters are connected to the system. Thus, they should be modeled in the earth fault simulations.

The modeling of the OWF components should be performed based on the frequency range of the phenomena and time interval of study. The WTTs, for the initial time interval after energization or ground fault, are modeled based on the high frequency behavior. VCBs have multiple prestrike and multiple reignitions in energization and de-energization respectively, which can significantly affect the amplitude and waveform of overvoltages in OWF [2]. However, since the

focus of this paper is on resonant overvoltages at the LV terminal, VCBs are simply modeled as ideal switches. The platform transformer is modeled with the typical saturable 50 Hz transformer model. In sub-sections A-E, the component models are described in detail.

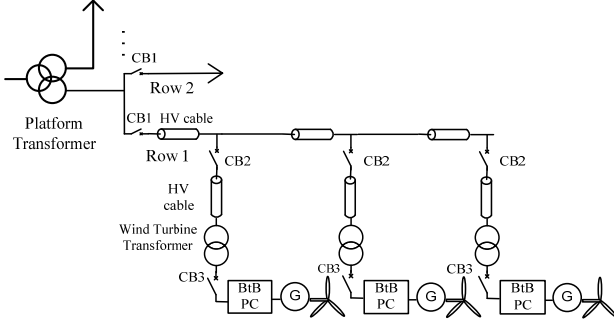


Fig. 1. The layout of typical offshore wind farms

A. Wind turbine transformer

For representing the 300 kVA transformer in ATP-EMTP, we used a wide-band model of the transformer developed in [9]. Here, the following steps were taken.

1. The 6×6 admittance matrix of 11.4/0.23 kV, 300 kVA transformer was established by measurements as a function of frequency from 10 Hz to 10 MHz. The coaxial measurement cables were compensated for.
2. A six-terminal black box model of the transformer on pole-residue form was obtained based on vector fitting [10]-[11] followed by passivity enforcement by residue perturbation.
3. An equivalent RLC lumped network was generated from the rational model and implemented in ATP-EMTP.

Fig. 2 shows the transferred voltage to LV for the transformer model. The transferred voltage is maximum at 2 MHz and this is denoted the dominant resonance frequency (f_{dr}).

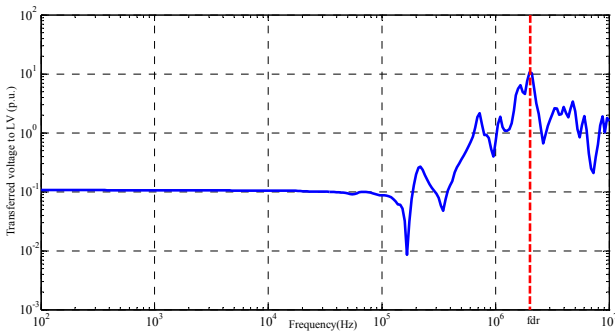


Fig. 2. The transferred voltage to LV for 300 kVA transformer in p.u. HV

B. Power Converter model with both GSC and MSC

In this model, the wind turbine has two Voltage Source Converters (VSC) connected in back to back configuration (see Fig. 3). The control and the operation of the converters

are based on the modeling and control design discussed in [12].

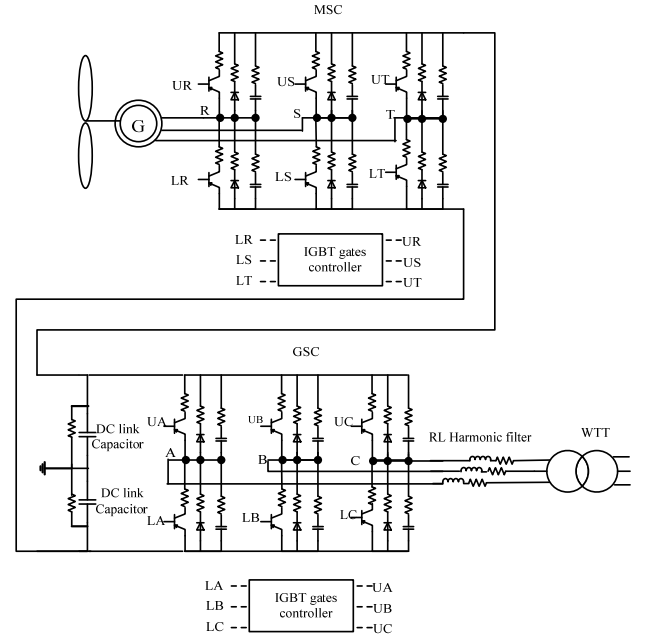


Fig. 3. Wind turbine with back to back full-scale converter and transformer

The VSC connected to the generator is referred to as the Machine Side Converter (MSC) and the second converter connected to the WTT through RL harmonic filters is referred to as the grid side converter (GSC). In order to study the transient behavior in this paper, the generator is modeled as an ideal source behind impedance. Switched converters along with detailed control systems are model for both the MSC and the GSC. A set of three phase Pulse Width Modulated (PWM) switching signals is obtained from the converter control system and applied to the switches in the converter. In the present work, the MSC controls the DC bus voltage. The GSC controls the reactive and the active power fed into the collection system. Fig. 4 shows the controller block diagram for decoupled active and reactive power control of the converter. In the transient simulation, a $0.03 \mu\text{s}$ time step is used. The converter control system is implemented as a MODELS code for the studies reported in this paper. To speed up the simulation, the MODELS code is executed with an increased (down sampled) time step of 10 microseconds, reasonably adapted to the time constants of its input signals.

As the simulations is still time consuming, a model valid and adequate only for the short time interval ($<10 \mu\text{s}$) during resonant transients is introduced in next subsection. The simulation time with same computing machine drops from couple of minutes to seconds.

IGBTs in both MSC and GSC have 6 different switching positions (sequences). For the GSC, they are listed in table I. For instance in seq. 1, LA, UB and LC are on and phase A and C are connected together and via DC link capacitor connected to phase B. RC snubber circuits parallel to each IGBT in Fig. 3 are protecting them from high voltage variations. RL harmonic filters are used to smooth the output of GSC during

steady state and decrease harmonics [13]. The typical values of these four elements and DC link capacitor and its parallel resistance are listed in table II.

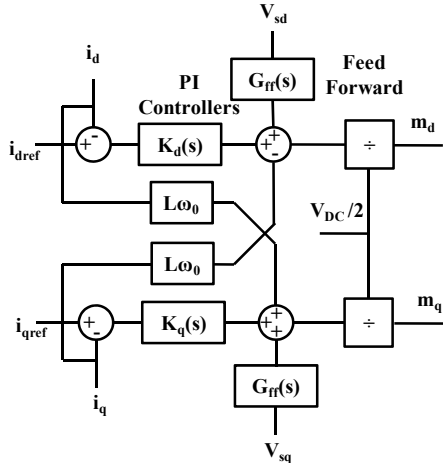


Fig.4. Converter control block diagram

TABLE I
SPECIFICATION OF IGNITED SWITCHES IN GSC IN EACH SEQUENCE

Seq. 1	LA	UB	LC
Seq. 2	UA	UB	LC
Seq. 3	UA	LB	LC
Seq. 4	UA	LB	UC
Seq. 5	LA	LB	UC
Seq. 6	LA	UB	UC

*L and U are abbreviation of Lower switch and Upper switch.
* A,B and C are phases.

TABLE II
TYPICAL VALUES OF RC SNUBBER AND RL FILTER

parameters	value
RC snubber in GSC	100Ω, 2μF
RC snubber in MSC	1000Ω, 0.2μF
RL harmonic filter	0.4mΩ, 2.3μH
DC link RC	10kΩ, 16 mF

C. Power Converter model with GSC and DC link capacitor

When an single phase earth fault occurs at the peak of phase A and GSC is in operation, the IGBTs would be in one of the 6 different switching positions (sequences) listed in table I. since the duration of resonant overvoltages is typically 5-10 μs. It should be mentioned that in this model, the DC link capacitor is considered passive and charged. During this time interval, the power production does not change and DC link capacitor functions only as filter for resonant transients. Meanwhile, MSC and generator are not considered. This model is only valid for resonant transient studies.

D. Cable Modeling

The JMarti model [14] is used to model interconnecting cables in OWF. This model considers the modal transformation matrix as real and fixed. It can be computed at a user-

defined frequency. In this paper, it is considered to be equal to the cable quarter-wave resonance frequency (1). Such modeling is valid for single core cables at high frequencies since all waves propagate essentially as coaxial waves. In the case of a single cable that is subjected to a step voltage on one end, the open-end voltage response has a dominant frequency at the cable quarter-wave resonance frequency,

$$f_s = \frac{1}{4\tau} = \frac{v_{cable}}{4l} = \frac{c}{4l\sqrt{\epsilon_r}} \quad (1)$$

v_{cable} for high frequencies is defined inversely proportional to the square root of relative permittivity (ϵ_r) of the cable insulation. The speed of light in vacuum is denoted with c . The single core cable parameters used in this paper is shown in table III. In order to verify the cable and WTT model, the experimental energization circuit in [9] was simulated (see Fig. 5) and the LV resonant overvoltages were reproduced in good agreement (see Fig. 6).

TABLE III
HV CABLE PARAMETERS

core outer radius (m)	0.02
core resistivity (ohm×m)	1.72×10^{-8}
Relative core-sheath insulation permittivity	2.671
sheath inner radius (m)	0.035
sheath outer radius (m)	0.038
sheath resistivity (ohm×m)	2.2×10^{-7}
Relative sheath insulation permittivity	2.3

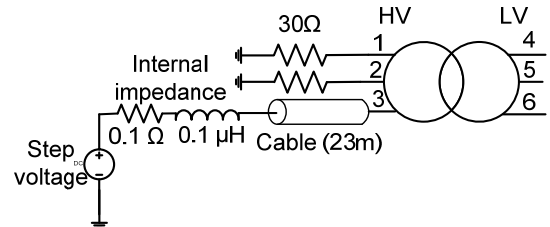


Fig.5. one phase energization with 23 m cable in accordance with Fig. 14 in [9].

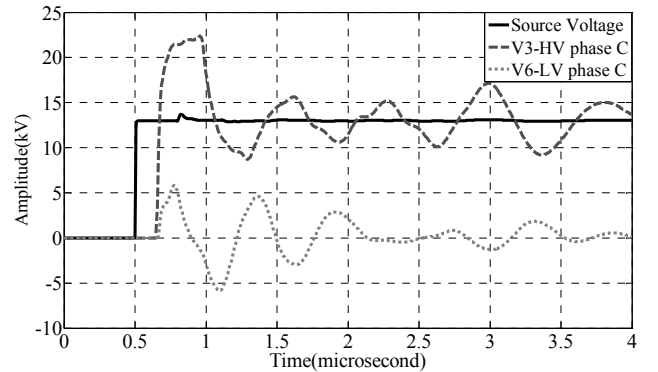


Fig.6. Verification of cable modeling according to Fig. 5. Source voltage (solid line), voltage on phase C HV terminal (dashed line), voltage on phase C LV terminal (dotted line).

E. RC Filters

RC filters can be applied at both LV and HV terminals of a WTT for controlling overvoltages; especially du/dt . The selection of RC values should be done based on both transient and steady state situations. $R=10\Omega$ and $C=500\text{ nF}$ are used for HV and LV filters in this paper, leading to $P_{3\text{phase}}=13\text{mW}$ and $Q_{3\text{phase}}=8\text{VAr}$ which are well ignorable values for steady state situation. Series stray inductances of $0.25\ \mu\text{H}$ are introduced for representing the ground lead in HV and LV RC filters. This inductance decreases the efficiency of RC filter and should be minimized. In next section, the effect of them will be analyzed.

F. Surge Arrester

Generally, Surge Arresters (SA) are installed at HV and LV terminals of transformers to protect them from lightning surges which strike the wind turbine blades or nacelle [15]. In this paper, the non-linear and frequency dependent model introduced by IEEE working group in [16] is applied. The characteristics of SA applied at LV and HV terminals of the WTT are based on [17] and [18], respectively. Series stray inductances of $0.5\ \mu\text{H}$ and $0.25\ \mu\text{H}$ are introduced for representing the ground lead in HV and LV SAs, respectively.

III. SIMULATION RESULTS

In this section, simulation results for both wind turbine energization and single phase earth fault are reported. Since protective devices and their design are going to be analyzed and compared in this section, there should be criteria for the selection of adequate protection.

For LV equipment, the accepted $1.2/50\mu\text{s}$ impulse overvoltages with $V_{\text{peak}} < 300\text{V}$ is 4 kV according to Table B.1 in IEC 60664-1. This permits impulse overvoltages up to 21 p.u. and du/dt up to $21/1.2=17.5\text{ p.u./}\mu\text{s}$ to be acceptable for LV terminal of WTTs. Meanwhile, depending on dominant resonance frequency, f_{dr} , and the availability of critical voltage vs. rise time, the typical value of rise time can be assumed as $1/(4f_{dr})$ and the critical voltage for that rise time can be considered for more accuracy. In [7], the measured critical voltage envelope vs. rise time for a 34.5 kV , 200 kVA transformer decreases by shorter rise times such as for 50 ns rise time, the critical voltage reduces to 1 p.u. Thus, $1/0.05=20\text{ p.u./}\mu\text{s}$ is the critical du/dt which is in good agreement with the aforementioned standard value. Fig. 7 shows the layout of possible protective devices installed at WTT terminals.

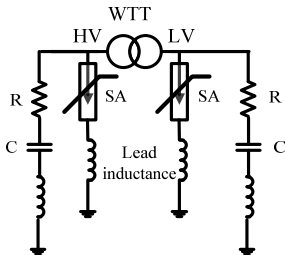


Fig.7. Installation of RC filter and surge arresters on LV and HV terminal of WTT.

A. Wind turbine energization

Fig 1. shows the layout of OWF when WTT is on top of nacelle. In fact, it can also be installed in the base. Thus, the energization can directly be done on the HV terminal. In this paper, energizations occur at the peak voltage of phase A. Figs 8 and 9 show the induced voltage on the LV terminal for various protection schemes when the transformer is in the base or on top of nacelle, respectively. Having no protection, the amplitude of the overvoltages (blue waveforms in Figs 8 and 9) are 12 p.u., which is well within safe margin. The quarter wave frequency of the HV cable (length=23 m) is equal to dominant resonance frequency of WTT (2MHz) and leads to resonant overvoltages in Fig. 9 which persist for longer time (in this case double duration) compared to energization at HV terminal. On the other hand, the energization of the transformer in the base has slightly higher du/dt compared to resonant overvoltages (see table. IV).

According to Figs 8 and 9 and table IV, the existence of stray series inductances results in less affectivity of protective devices. For example, inductance-free (ideal) RC filters at LV terminal can diminish both overvoltage amplitude and du/dt to safe levels (acceptable $du/dt=17.5\text{ p.u./}\mu\text{s}$). Comparing the protection options in table IV, RC filters at both HV and LV terminal, which have low series impedance (in this case $0.25\mu\text{H}$) can compensate the negative effect of series inductance and decrease the du/dt to safe margin. In [19], it is shown that even during energization of the second WTT in a row, there is a potential of resonant overvoltage induction on LV terminal of the first WTT. In that case, the RC filters also are adequate protective devices.

B. Earth Fault in the wind farm

As analyzed in previous sub-section, for this 300 kVA WTT, the switching at the peak of phase A with 23 m cable length leads to resonant overvoltages at LV terminal. That is also valid for earth fault since it can be interpreted as switching at the peak of phase A to ground potential. WTT can be on the top of nacelle or at the base. Therefore, earth fault scenarios which can lead to resonant overvoltage are different (see Fig.10).

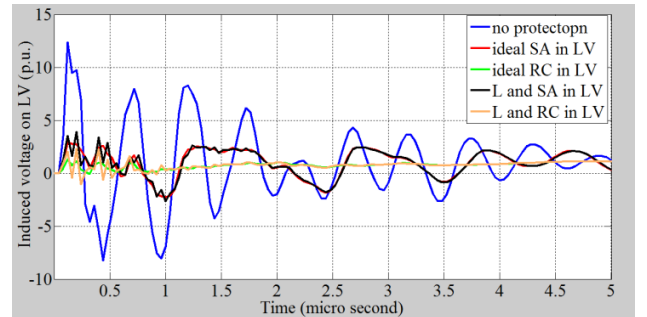


Fig.8. Induced voltage on the LV terminal of first WTT in Fig.1 when it is in the base with various protection devices at LV side (L and SA means surge arrester with inductive lead).

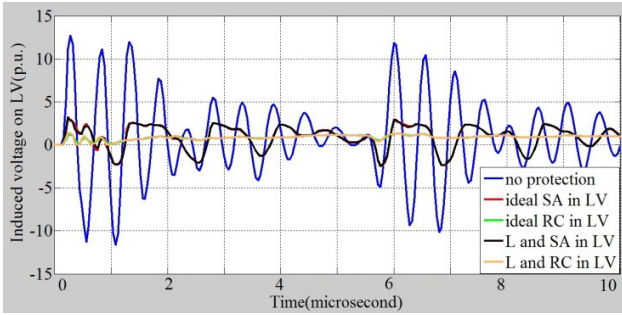


Fig.9. Induced voltage on the LV terminal during energization of first WTT in Fig.1 when it is on top of nacelle.

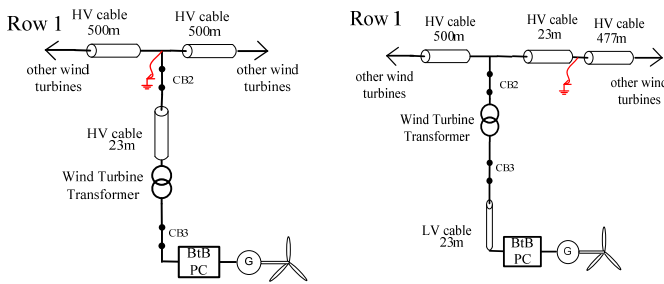


Fig.10. resonant overvoltage due to earth fault. left: WTT on top of nacelle, right: WTT in the base.

TABLE IV
RATE OF RISE/FALL OF VOLTAGE (P.U./ μ S) FOR VARIOUS PROTECTION SCHEMES INCLUDING RESULTS IN FIGS. 8 AND 9.

Protective devices	WTT in the base	WTT on the nacelle
No protection	154	93
SA(LV) with L*	44	27
Ideal SA(LV)	36	25
RC(LV) with L*	25	11
Ideal RC(LV)	16	9.5
SA(LV) & RC(LV)*	20	11
SA(LV),RC(LV) & SA(HV)*	19	10
SA(LV),RC(LV),SA(HV) & RC(HV)*	13	4
RC(LV) & RC(HV)*	16	4.5

*In this cases, stray series inductance is included to protective devices.

Fig. 11 shows the comparison between the two models for induced overvoltages to LV phase A due to single phase earth fault in the base (Fig. 10-left). The simulation results for both models are in good agreement. It can be concluded that the PC model with GSC and DC link capacitor is adequately accurate for resonant transient studies. It should be mentioned that all IGBT sequences in the latter model results in the same transient result. The simulation results of both models had dc biases due to fixed voltage at DC link capacitor, which are subtracted for easier comparison. When the middle point of DC link capacitor is not grounded, the resonant transient is more persistent. The peak-to-peak of overvoltages in GSCs with grounded and ungrounded DC link middle points are 12 and 18 p.u., respectively. The maximum value of du/dt equals

to 70 for both cases.

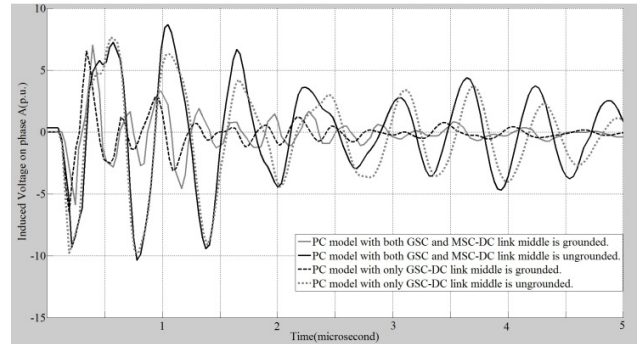


Fig.11. Induced voltage on the LV terminal for the scenario in Fig. 10-left

Since ungrounded DC link leads to more severe resonant transients, it is further analyzed in this paper. Besides, the model with GSC and DC link capacitor is applied. Fig. 12 shows the induced voltage on the LV terminal during earth fault for the two scenarios in Fig. 10. When WTT is in the nacelle and earth fault occurs in the base (cable length=wind turbine height=23m), the first transient surge arriving at the transformer is double compared to when WTT is in the base and earth fault occurs in 23 m distance in row cable. In the former case, the first surge meets the HV input impedance of WTT, which is high. While in the latter case, it meets the equivalent impedance of the transformer and other HV cables, which approximately equals to the surge impedance of the HV cable.

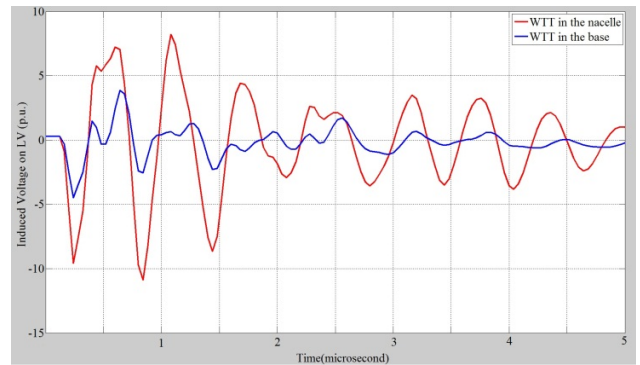


Fig. 12. Induced voltage on the LV terminal for two earth fault scenarios in Fig. 10 when the DC link middle point is ungrounded and GSC has seq.1.

Earth faults for WTT on the top of nacelle are now further investigated. Since, it is more critical than other scenario. If earth fault in resonance condition occurs when GSC is not connected, the highest overvoltage will be induced at the LV terminal of WTT (30 p.u. and 400 p.u./ μ s). Earth fault at the peak of phase A in critical cable length (in this case 23 m) with low earth fault impedance results in persistent resonance oscillations at the LV terminal. The red waveforms in Figs 13-15 show the induced voltage on phases A, B and C for this situation. According to the simulation results in Figs 13-15, the voltages of each phase are almost the same regardless to the IGBT switching sequences. Thus, we analyze the effect of components in GSC, RL harmonic filter and RC filters at LV and HV terminal only for one sequence, e.g. seq. 1.

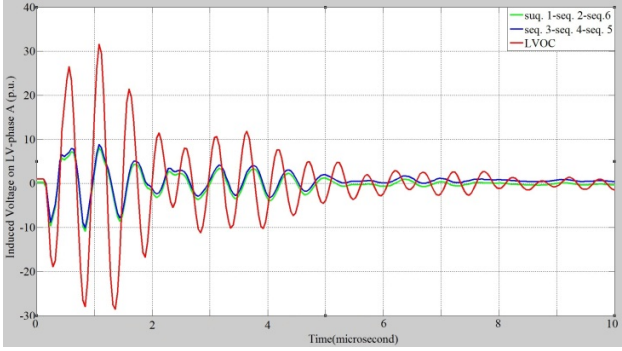


Fig. 13. Induced voltage on LV-phase A for earth fault at peak phase A for the scenario in Fig. 10-left with converter in various sequences according to table I or LV open circuit.

As shown in Fig. 13, the amplitude and du/dt of the induced voltage are decreased to one-third on LV when the GSC is connected. The reason can be explained in this way: seq. 1 can be interpreted with good approximation as a short circuit between phase A and C and other sequences has other kind of two phase short circuits. This short circuit effects the transformer terminal connection and consequently the transients.

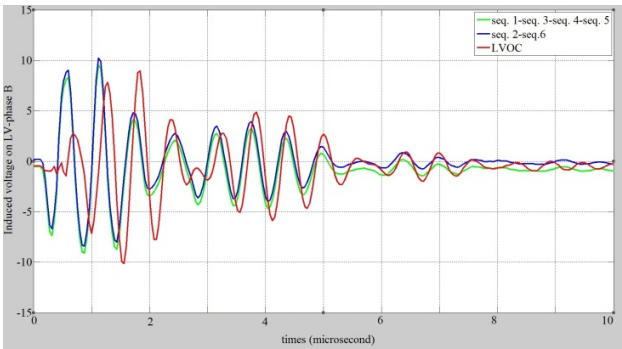


Fig. 14. Induced voltage on LV-phase B for earth fault at peak phase A for the scenario in Fig. 10-left in various sequences in table I and LV open circuit.

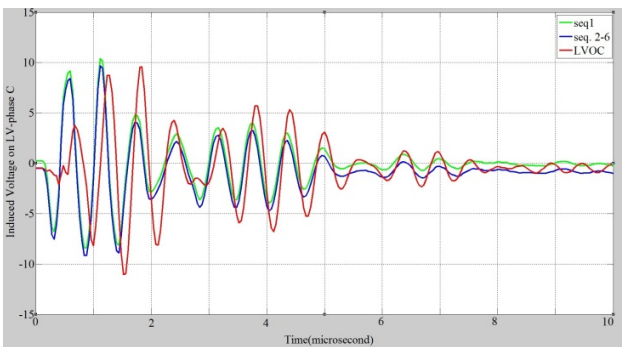


Fig. 15. Induced voltage on LV-phase C for earth fault at peak phase A for the scenario in Fig. 10-left in various sequences in table I and LV open circuit.

The main component with dominant effect on overvoltage transients at the LV terminal is the RL harmonic filter. Fig. 16 shows that the increase of the inductance leads to the increase of the overvoltage amplitude and du/dt . However, four times increase of the DC link capacitor or the capacitors in RC snubber circuits do not change the transients effectively.

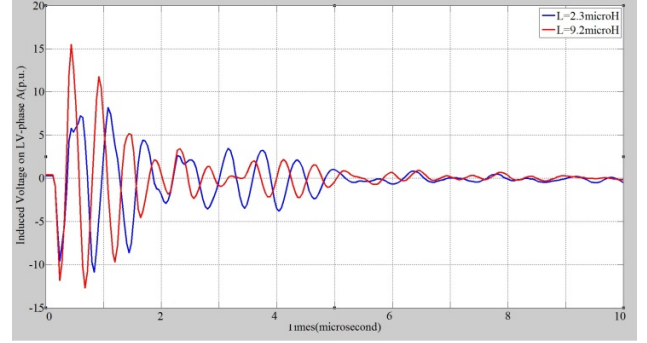


Fig. 16. The effect of L in RL harmonic filter on the induced voltage on LV-phase A.

Installing RC filter ($R=10\Omega$ and $C=500$ nF) at LV and HV with low stray inductance ($0.25 \mu\text{H}$) results in similar induced voltage on LV as in Fig. 9. The amplitudes decrease to 1 and 0.5 p.u. for uninitiated and initiated GSC, respectively. Besides, du/dt decrease to 10 and 5 p.u./ μs , respectively. This means that the application of just RC filter protects the LV terminal of WTT and GSC components effectively.

IV. CONCLUSIONS

In this paper, the resonant overvoltages at LV terminal of wind turbine transformers due to energization or single phase earth fault in feeder cables are analyzed. Both energization and earth fault are considered to occur at the peak of phase A. It was found that if the lengths of energizing cable or cable distance of earth fault are such that their quarter wave frequencies are equal to one of resonance frequencies of the transformer, resonant overvoltages occur. In this paper, the highest resonant overvoltages occurs (30 p.u.) for earth fault in 23 m cable distance from the wind turbine transformer if grid side converter is not connected. Since single phase earth fault at peak of phase A can be interpreted as energization of negative voltage source with very low internal impedance (short circuit impedance). This creates more sustained oscillations and large induced voltage on LV side.

If earth fault occurs at the peak of phase A during power production by generator, the inductance in the series RL harmonic filter dominantly affect the resonant transients. The amplitude of resonant overvoltages and du/dt increases with higher inductances.

Simulation results also show that installation of wind turbine transformers in the base leads to relatively less vulnerable resonant overvoltages compared to transformer in the nacelle. It was found that installation of RC filters at both HV and LV terminal, which are inductance-free or has adequately low stray inductance, protects the LV terminal of WTT from resonant overvoltages due to both energization and earth fault.

V. ACKNOWLEDGMENT

Authors greatly appreciate Norwegian Research Center for Offshore Wind Technology (NOWITECH) which is sources of funding.

VI. REFERENCES

- [1] I. Arana, A. Hernandez, G. Thumm, and J. Holboell, "Energization of wind turbine transformers with an auxiliary generator in a large offshore wind farm during islanded operation", *IEEE Trans. Power Delivery*, vol. 26, no. 4, pp. 2792-2800, Oct. 2011.
- [2] L. Liljestrand, A. Sannino, H. Breder, and S. Thorburn, "Transients in collection grids of large offshore wind parks," *Wiley Inter science*, vol. 11 Issue 1, Pages 45 – 61, 2008.
- [3] I. Arana, J. Holbøll, T. Sørensen, A. H. Nielsen, P. Sørensen, and O. Holmstrøm, "Comparison of measured transient overvoltages in the collection grid of Nysted offshore wind farm with EMT Simulations", in *proc. 2009 International Conference on Power Systems Transients (IPST)*, paper 38.
- [4] C.D. Tsirekis, G.J. Tsekouras, N.D. Hatziaargyriou, B.C. Papadias, "Investigation of switching transient effects on power systems including wind farms", in *proc. 2001 IEEE Powertech conference*, vol 4.
- [5] V. Akhmatov, B. C. Gellert, T. E.McDermott, W. Wiechowski, "Risk of temporary over-voltage and high-voltage fault-ride-through of large wind power plant", in *Proc. 2010 9th Int. Workshop on Large-Scale Integration of Wind Power into Power Systems*.
- [6] B. Badrzadeh, M. Høgdahr, N. Singh, H. Breder, K. Srivastava, M. Reza, "Transient in wind power plants- part II: case studies", *IEEE Trans. Industry Applications*, vol. 48, no. 5, Sep.-Oct. 2012.
- [7] T. Abdulahovic, "Analysis of High-Frequency Electrical Transients in Offshore Wind Parks." Ph.D. dissertation, Dept. Energy and Environment, division of electric power eng., Göteborg : Chalmers University of Technology, 2011..
- [8] B. Badrzadeh, B. Gustavsen, "High frequency modeling and simulation of wind turbine transformer with doubly fed asynchronous generator", *IEEE transaction on Power Delivery*, vol. 27, no. 2, pp. 746-756, 2012.
- [9] B. Gustavsen, "Study of transformer resonant overvoltages caused by cable-transformer high frequency interaction," *IEEE trans. Power Delivery*, vol. 25, no. 2, pp. 770-779, Apr. 2010.
- [10] B. Gustavsen, "Wide band modelling of power transformers," *IEEE transaction on Power Delivery*, vol. 19, No. 1, pp. 414-429, 2004.
- [11] B. Gustavsen and A. Semlyen, "Rational approximation of frequency domain responses by vector fitting," *IEEE trans. Power Delivery*, vol. 14, no. 3, pp. 1052-1061, 1999.
- [12] A. Yazdani and R. Iravani, *Voltage-Sourced Converters in Power Systems*. New York: IEEE/ Wiley, Feb 2010.
- [13] N. Mohan, T. M. Undeland, W. P. Robbins, *Electronics Converters, Applications and Design*, New York: Wiley, 1995.
- [14] J.R. Marti, "Accurate modeling of frequency-dependent transmission lines in electromagnetic transient simulations", *IEEE Trans. PAS*, vol. 101, no. 1, pp. 147-157, Jan. 1982.
- [15] Y. Yasuda, N. Uno, H. Kobayashi, and T. Funabashi, "Surge analysis on wind farm when winter lightning strikes", *IEEE Trans. Energy Conversion*, vol. 23, no. 1, pp. 257-262, 2008.
- [16] IEEE Working Group on Surge Arrester Modeling, "Modeling of metal oxide surge arresters," *IEEE trans. power delivery*, vol. 7, no. 1, pp. 302-309, Jan. 1992.
- [17] ABB surge arrester POLIM-R-2N datasheet[online]. Available: <http://www.abb.com/search.aspx?q=POLIM-R-2N&abbcontext=products>.
- [18] ABB surge arrester POLIM-C-N datasheet, [online]. Available: <http://www.abb.com/product/db0003db004279/c125739900636470c125708c003fd77a.aspx>.
- [19] A. H. Soloot, H. Kr. Hoidalén, B. Gustavsen, "The Assessment of Overvoltage Protection Within Energization of Offshore Wind Farms," *Energy Procedia*, vol. 24, pp. 151-158, 2012.